Supplemental Material to "Theory for Anomalous Terahertz Emission in Striped Cuprate Superconductors"

I. PLANE WAVES IN THE MEDIUM WITH STRIPES

Here we analyse plane waves in the sample with stripes. Because of the translational symmetry breaking along the z-axis, the structure of free harmonics contains the mixing between q_z and $q_z + Q$ wave vectors; at the same time, along the x-axis, we can substitute an evanescent wave ansatz:

$$B_{\mathrm{mat},y} = (\alpha e^{iq_z z} + \beta e^{i(q_z+Q)z})e^{-\lambda x - i\omega t}, \quad \text{(S1)}$$

where $\lambda(\omega, q_z)$ is yet unknown wave vector that depends on both ω and q_z; α and β are two coefficients that encode the strength of the mentioned mixing. Substituting this ansatz into the fourth Maxwell equation with the modified dielectric function, Eq. (8) of the main text, we obtain the electric field in the sample:

$$E_{\mathrm{mat},x} = \frac{c^2}{\omega\varepsilon_{ab}}\Big[q_z\alpha e^{iq_z z} + (q_z+Q)\beta e^{i(q_z+Q)z}\Big]e^{-\lambda x - i\omega t},$$

$$E_{\mathrm{mat},z} = -\frac{ic^2\lambda\varepsilon_c}{\omega(\varepsilon_c^2 - A^2)}\Big[\Big(\alpha - \frac{A}{\varepsilon_c}\beta\Big)e^{iq_z z} + \Big(\beta - \frac{A}{\varepsilon_c}\alpha\Big)e^{i(q_z+Q)z}\Big]e^{-\lambda x - i\omega t}.$$

Plugging this result into the third Maxwell equation, we get the following secular equation:

$$\begin{bmatrix} k_m^2(q_z,\omega) - \lambda^2 & A\lambda^2/\varepsilon_c \\ A\lambda^2/\varepsilon_c & k_m^2(q_z+Q,\omega) - \lambda^2 \end{bmatrix}\begin{bmatrix}\alpha\\ \beta\end{bmatrix} = \begin{bmatrix}0\\0\end{bmatrix}, \quad \text{(S2)}$$

where $k_m(q,\omega)$ is determined implicitly through

$$\frac{q^2}{\varepsilon_{ab}} - \frac{k_m^2(q,\omega)\varepsilon_c}{\varepsilon_c^2 - A^2} = \frac{\omega^2}{c^2}. \quad \text{(S3)}$$

For consistency, when solving this equation, we choose the root with $\mathrm{Re}\, k_m(q,\omega) > 0$. There are four eigenvalues of Eq. (S2):

$$\lambda = \pm\sqrt{\frac{k_m^2 + \tilde{k}_m^2 \pm \sqrt{(k_m^2+\tilde{k}_m^2)^2 - 4k_m^2\tilde{k}_m^2\Big(1 - \frac{A^2}{\varepsilon_c^2}\Big)}}{2\Big(1 - \frac{A^2}{\varepsilon_c^2}\Big)}},$$

where we defined $\tilde{k}_m = k_m(q_z+Q,\omega)$. We select the two of them with $\mathrm{Re}\,\lambda_1, \mathrm{Re}\,\lambda_2 > 0$ that describe waves decaying into the sample. We choose these roots such that in the limit $A \to 0$, we get $\lambda_1 \approx k_m$ and $\lambda_2 \approx \tilde{k}_m$. Equation (S2) also fixes the ratio between the amplitudes α and β:

$$\bar{\gamma}_\lambda \equiv \gamma_\lambda^{-1} \equiv \frac{\alpha}{\beta} = \frac{\lambda^2}{\lambda^2 - k_m^2}\frac{A}{\varepsilon_c} = \frac{\lambda^2 - \tilde{k}_m^2}{\lambda^2}\frac{\varepsilon_c}{A}. \quad \text{(S4)}$$

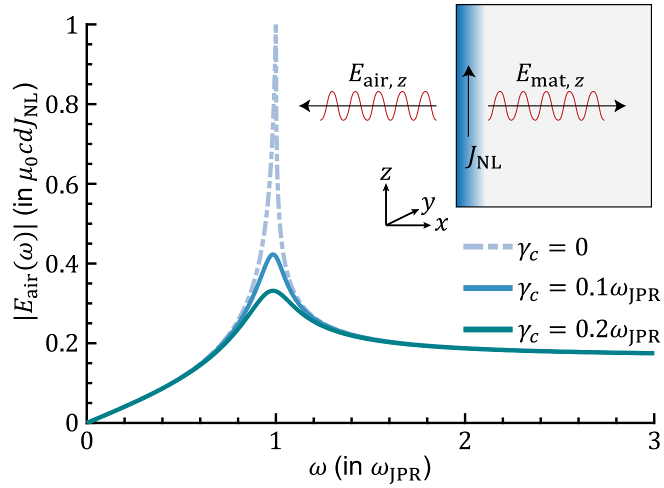

FIG. S1. Bulk polariton scenario. While the photocurrent in Eq. (1) does not depend on frequency ω, for $\omega \lesssim \omega_{\mathrm{JPR}}$, we find that the amplitude of the radiation into the air displays a peak at ω_{JPR}. This peak, though, is smeared out for realistic values of the quasiparticle damping γ_c. The inset illustrates that the photocurrent serves as a drive that emits radiation into the air and the superconductor.

II. BULK POLARITON SCENARIO

In this section, we consider a simplified phenomenological model, where we assume the presence of a broadband photocurrent, Eq. (1) of the main text, but we neglect stripes and do not take into account how they modify the dielectric properties of the sample. This is a bit artificial because the photocurrent generation itself is expected to occur due to the stripes [16]. Nevertheless, this approach allows us to separate the response due to the bulk Josephson plasmons from the surface modes since the latter remain silent because they lie outside the light cone, as shown in Fig. 1(a) of the main text. In other words, the emission we compute below comes entirely due to the bulk excitations.

To get the emission properties in this model, we first solve the Maxwell equations in each media. In the air, we have an outgoing plane wave, which we write as:

$$B_{\mathrm{air},y} = B_a e^{-i\omega x/c - i\omega t},\; E_{\mathrm{air},z} = cB_a e^{-i\omega x/c - i\omega t}, \quad \text{(S5)}$$

where $B_a(\omega)$ encodes the amplitude of this plane wave. In the superconductor, the solution reads:

$$B_{\mathrm{mat},y} = B_m e^{iq_m x - i\omega t}, \quad \text{(S6)}$$

where $q_m(\omega)$ is yet an unknown wave vector that depends on ω, and $B_m(\omega)$ is the amplitude of this medium harmonic. From the fourth Maxwell equation, we obtain the electric field in the sample:

$$E_{\mathrm{mat},z} = -\frac{q_m c^2}{\omega \varepsilon_c} B_m e^{iq_m x - i\omega t}. \tag{S7}$$

By plugging this into the third Maxwell equation, we get: $q_m^2 = \omega^2 \varepsilon_c(\omega)/c^2$. Now, using the generalized Fresnel boundary conditions, derived in the main text, we finally obtain:

$$B_a(\omega) = -\frac{\mu_0 d J_{\mathrm{NL}}}{1 + \sqrt{\varepsilon_c(\omega)}} = f(\omega)\mu_0 d J_{\mathrm{NL}}. \tag{S8}$$

This is the central result of this section, which we turn to discuss in detail.

Figure S1 shows the amplitude $f(\omega)$ of the emitted into the air radiation as a function of frequency ω. We find that even though the photocurrent is flat for $\omega \lesssim \omega_{\mathrm{JPR}}$, $f(\omega)$ is peaked at ω_{JPR}, i.e., the superconductor acts a low-frequency filter to the featureless drive $J_{\mathrm{NL}}(\omega)$. The reason for this peaked behavior is the enhanced due to the van Hove singularity density of states of bulk c-axis Josephson plasmons at $\omega = \omega_{\mathrm{JPR}}$. We now turn to discuss the dependence of $f(\omega)$ in more detail. First, at large frequencies $\omega \gtrsim \omega_{\mathrm{JPR}}$, where the photon dispersion inside the sample (bulk polariton) becomes approximately linear, the drive can emit light into both the air and the material. The fraction of how much it emits into the air is entirely determined by the relative speed of light $c/c_m = \sqrt{\varepsilon_{\infty,ab}}$ in the air to that in the superconductor. For instance, in case $c = c_m$, half of the radiation would go into the air and the other half into the sample. Second, for small frequencies $\omega \to 0$, we find that $f(\omega)$ becomes suppressed and, in particular, $f(0) = 0$. The reason for this is that fundamentally, the superconductor can easily screen dc current, not allowing a low-frequency electric field to develop.

We comment that the peak at ω_{JPR} can be smeared out by finite γ_c. For realistic parameters, this smearing effect is profound, and the resulting emission spectrum is too broad to explain the experiment [16]. In contrast, the surface scenario provides sharp emission even if γ_c is notable essentially because the Umklapp photocurrent *resonantly* drives the surface modes.

We turn to discuss an additional argument why the bulk scenario is inconsistent with the experimental phenomenology. In the experiment [16], the emission was detected in two LBCO samples corresponding to two different dopings. These samples have stripes with different relative strengths and out-of-plane coherence lengths, and the resulting emission was more intense and much narrower in frequency for the sample with stronger, more coherent stripes. The issue with the bulk scenario, however, is that the far-field reflectivity, which entirely determines the emission properties associated with the bulk modes, is known to be insensitive to the stripes [16, 57]. Therefore, the bulk plasmons are expected to produce similar radiation in the two samples, with the same lineshapes independent of the stripe correlation length and, thus, disagreeing with the experiment. In contrast, the emission from the surface Josephson plasmons is acutely sensitive to the CDW order, further justifying our expectation that the observed phenomenon comes from the surface modes.

III. SURFACE JOSEPHSON PLASMONS AT LARGE MOMENTA

In the main text, we considered bulk c-axis Josephson plasmons with flat dispersion, as encoded in momentum-independent electric permittivity (3). If one is interested in small momenta close to the light cone $q \simeq \omega/c$, then this approach is well-justified. However, we also encountered in the main text the situation of Bragg mixing of surface modes with small momenta to those that have large momenta $q \simeq Q_{\mathrm{CDW}}$. For these latter modes, it might be essential to consider the momentum dependence of $\hat{\varepsilon}(\omega, q)$, as we do in this section. On the phenomenological level, the leading correction to the flat c-axis dispersion comes from the effects of quasiparticle compressibility, which, in turn, sets a very large Thomas-Fermi momentum scale q_{TF}. We expect that in cuprates $Q_{\mathrm{CDW}} \lesssim q_{\mathrm{TF}} \lesssim 2\pi/a_0$, implying that: i) Q_{CDW} is still small enough so that one can essentially disregard momentum dependence of $\hat{\varepsilon}(\omega, q)$ for $q \lesssim Q_{\mathrm{CDW}}$; ii) the lattice reciprocal momentum $2\pi/a_0$ is large, and effects of compressibility cannot be ignored at such a momentum scale [59]. In the literature, the dispersions of the usual surface plasmons and the surface Josephson plasmons in stacked 2D metals and anisotropic superconductors have been discussed in various geometries, including infinite half-space, thin film [60], and spherical particles [61]. In our theory, we go beyond previous treatments of surface Josephson plasmons by including the effects of quasiparticle compressibility, which allows us to capture the dispersion of surface excitations at large momenta of the order of Q_{CDW}.

We describe the electric response of superconductors within the two-fluid model [62], where the total electric current $\boldsymbol{J} = \boldsymbol{J}_n + \boldsymbol{J}_s$ is represented as a sum of the quasiparticle contribution $\boldsymbol{J}_n$ and the one due to the superflow $\boldsymbol{J}_s$. For the normal component, we write Ohm's law but take into account the effects of electrochemical potential $\delta\mu = \delta\rho/\chi$, where $\delta\rho$ represents the electric charge density and χ is the compressibility:

$$\boldsymbol{J}_n = \hat{\sigma}(\boldsymbol{E} - \nabla\delta\mu). \tag{S9}$$

For simplicity, we assume that the quasiparticle conductivity tensor $\hat{\sigma} = \mathrm{diag}(\sigma_{ab}, \sigma_{ab}, \sigma_c)$ is frequency and momentum independent. For the superconducting part, we write London's equation:

$$\partial_t \boldsymbol{J}_s = \hat{\Lambda}(\boldsymbol{E} - \nabla\delta\mu). \tag{S10}$$

Within the BCS theory, the tensor $\hat{\Lambda} = \mathrm{diag}(\Lambda_{ab}, \Lambda_{ab}, \Lambda_c)$ is proportional to $|\psi|^2$, where ψ is the superconducting order parameter. We also have the continuity equation:

$$\partial_t \delta\rho + \nabla \cdot \boldsymbol{J} = 0. \tag{S11}$$

Using $\varepsilon_0 \nabla \cdot \boldsymbol{E} = \delta\rho$ and $\nabla \times \boldsymbol{B} = \mu_0(\boldsymbol{J}_n + \boldsymbol{J}_s) + \partial_t \boldsymbol{E}/c^2$, we evaluate the dielectric tensor of the material:

$$\hat{\varepsilon}_{\alpha\beta}(\boldsymbol{q}, \omega) = \varepsilon_\alpha \delta_{\alpha\beta} + (\varepsilon_\alpha - 1)\frac{q_\alpha q_\beta}{q_{\mathrm{TF}}^2}, \tag{S12}$$

where

$$\varepsilon_\alpha = 1 - \frac{\omega_\alpha^2}{\omega^2} + \frac{i\gamma_\alpha}{\omega}. \tag{S13}$$

Here we used that $\Lambda_\alpha = \varepsilon_0 \omega_\alpha$ and $\sigma_\alpha = \varepsilon_0 \gamma_\alpha$ and defined the Thomas-Fermi momentum as $q_{\mathrm{TF}}^2 = \chi/\varepsilon_0$. Equation (S12) implies that the c-axis Josephson plasmon dispersion is no longer flat: $\omega_c^2(q_z) = \omega_{\mathrm{JPR}}^2(1 + q_z^2/q_{\mathrm{TF}}^2)$. In the limit $q_{\mathrm{TF}} \to \infty$, we reproduce the result in Eq. (3), up to unimportant for this discussion anisotropy factors.

We turn to investigate plane waves in this dispersive medium and plug in the usual ansatz:

$$\boldsymbol{B} = B_y \hat{y}\, e^{iq_x x + iq_z z - i\omega t}, \tag{S14}$$

$$\boldsymbol{E} = (E_x \hat{x} + E_z \hat{z}) e^{iq_x x + iq_z z - i\omega t}. \tag{S15}$$

Using the third and fourth Maxwell equations, we obtain an implicit equation on $q_x(q_z, \omega)$: $\det \mathcal{M}(q_z, \omega) = 0$, where $\mathcal{M}$ is a 2×2 matrix given by

$$\begin{bmatrix} \varepsilon_{ab} - \dfrac{q_z^2 c^2}{\omega^2} + \dfrac{(\varepsilon_{ab} - 1) q_x^2}{q_{\mathrm{TF}}^2} & q_x q_z \Big[\dfrac{\varepsilon_{ab} - 1}{q_{\mathrm{TF}}^2} + \dfrac{c^2}{\omega^2}\Big] \\ q_x q_z \Big[\dfrac{\varepsilon_c - 1}{q_{\mathrm{TF}}^2} + \dfrac{c^2}{\omega^2}\Big] & \varepsilon_c - \dfrac{q_x^2 c^2}{\omega^2} + \dfrac{(\varepsilon_c - 1) q_z^2}{q_{\mathrm{TF}}^2} \end{bmatrix}.$$

This secular equation is only bi-quadratic in q_x. By solving it, we find four roots, out of which only two describe waves that decay into the sample ($q_x = ik_m$, so that $\mathrm{Re}\, k_m^{(1)}, \mathrm{Re}\, k_m^{(2)} > 0$). We choose these roots such that in the limit $q_{\mathrm{TF}} \to \infty$, the harmonic $k_m^{(1)}$ reduces to the result (5) of the main text:

$$[k_m^{(1)}]^2 = \varepsilon_c \Big(\frac{q_z^2}{\varepsilon_{ab}} - \frac{\omega^2}{c^2}\Big)\Big[1 - \frac{(\varepsilon_{ab} - \varepsilon_c)^2 q_z^2}{\varepsilon_c \varepsilon_{ab}^2 q_{\mathrm{TF}}^2} + \dots\Big]. \tag{S16}$$

Notably, as $q_{\mathrm{TF}} \to \infty$, the second root $k_m^{(2)} \sim q_{\mathrm{TF}}$ diverges, which essentially means that the second harmonic can be disregarded, as we elaborate below.

Our subsequent task is to study the surface collective excitations. Since for given q_z and ω, we have two distinct harmonics in the sample, we write the following ansatz:

$$B_z = e^{iq_z z - i\omega t} \begin{cases} B_0 e^{k_a x}, & x < 0 \\ B_1 e^{-k_m^{(1)} x} + B_2 e^{-k_m^{(2)} x}, & x > 0 \end{cases}. \tag{S17}$$

Amplitudes B_0, B_1, and B_2 are related to each through appropriate boundary conditions, which we turn to derive. From the first Maxwell equation, we obtain:

$$\varepsilon_0(E_{\mathrm{mat},x} - E_{\mathrm{air},x}) = \delta\rho_{\mathrm{2D}}, \tag{S18}$$

where $\delta\rho_{\mathrm{2D}}$ is the two-dimensional surface charge density, which we assume to be nonzero. Faraday's law gives:

$$E_{\mathrm{mat},z} = E_{\mathrm{air},z}. \tag{S19}$$

From Ampere's law, we obtain that the two-dimensional surface current flows along the z-axis, $\boldsymbol{J}_{\mathrm{2D}} \parallel \hat{z}$, which, in turn, gives:

$$B_{\mathrm{mat},y} - B_{\mathrm{air},y} = \mu_0 J_{\mathrm{2D},z}. \tag{S20}$$

By integrating the continuity equation (S11) near the surface, we finally get:

$$\partial_t \delta\rho_{\mathrm{2D}} + \partial_z J_{\mathrm{2D},z} + J_{\mathrm{mat},x} = 0. \tag{S21}$$

We note that the third term represents the 3-dimensional current density, reflecting the fact that the surface charge can leak into the bulk of the sample. To obtain a closed system of equations, we use the medium equations and find:

$$\mu_0 J_{\mathrm{mat},x} = -\frac{i\omega(\varepsilon_{ab} - 1)}{c^2}\Big[E_{\mathrm{mat},x} - \frac{\partial_x \partial_\alpha E_{\mathrm{mat},\alpha}}{q_{\mathrm{TF}}^2}\Big],$$

$$\mu_0 J_{\mathrm{2D},z} = -\frac{\omega q_z}{c^2 q_{\mathrm{TF}}^2}(\varepsilon_c - 1)[E_{\mathrm{mat},x} - E_{\mathrm{air},x}].$$

These medium relations, together with Eqs. (S17)-(S21), form a closed set of equations, which allows us to obtain the spectrum of the surface Josephson plasmons at arbitrary momenta.

While the above set of equations can be directly (numerically) solved, here we aim at understanding the effects of quasiparticle compressibility perturbatively, to the leading order in q_{TF}^{-2}. To this end, one can neglect the second strongly damped harmonic $k_m^{(2)}$ in Eq. (S17)

$$B_z = e^{iq_z z - i\omega t} \begin{cases} B_a e^{k_a x}, & x < 0 \\ B_m e^{-k_m^{(1)} x}, & x > 0 \end{cases}$$

and solve the following boundary problem:

$$E_{\mathrm{mat},z} = E_{\mathrm{air},z},$$

$$B_{\mathrm{mat},y} - B_{\mathrm{air},y} = -\frac{\omega q_z(\varepsilon_c - 1)}{c^2 q_{\mathrm{TF}}^2}[E_{\mathrm{mat},x} - E_{\mathrm{air},x}].$$

We remark that this perturbative approach satisfies the continuity equation (S21) to the leading order in q_{TF}^{-2}. In other words, the role of the harmonic $k_m^{(2)}$ is to satisfy the charge conservation at higher orders. For the spectrum of surface Josephson plasmons, we obtain the following approximate equation:

$$\frac{1}{k_a}\Big[1 + \frac{q_z^2(\varepsilon_c - 1)}{q_{\mathrm{TF}}^2}\Big] + \frac{\varepsilon_c}{k_m^{(1)}}\Big[1 + \frac{q_z^2(\varepsilon_c - 1)}{\varepsilon_c q_{\mathrm{TF}}^2}\Big] = 0. \tag{S22}$$

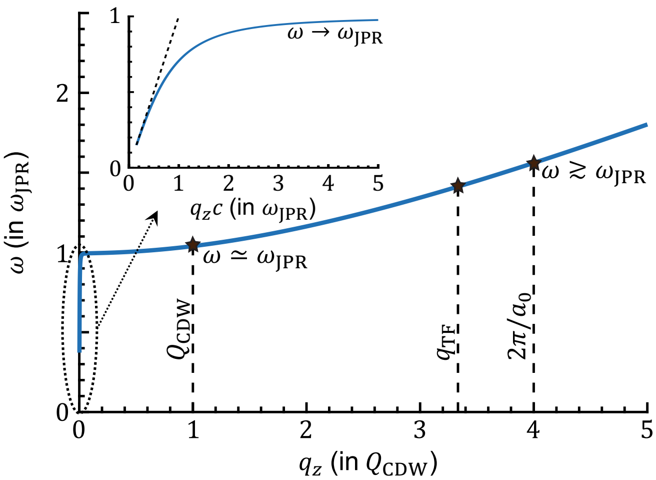

FIG. S2. Dispersion $\omega_s(q_z)$ of the surface excitations for large momenta $q_z \simeq q_{\mathrm{TF}}$, where the effects of quasiparticle compressibility become notable. In contrast to the behavior at low momenta near the light cone (inset), see also Fig. 1(a), where $\omega_s(q_z)$ displays a quick saturation near ω_{JPR}, now $\omega_s(q_z)$ is no longer flat. In cuprates, we expect $Q_{\mathrm{CDW}} \lesssim q_{\mathrm{TF}} \lesssim 2\pi/a_0$. In this case, the stripes momentum Q_{CDW} is still quite small, $\omega_s(Q_{\mathrm{CDW}}) \simeq \omega_{\mathrm{JPR}}$, and the effects of compressibility are unimportant at this scale. At the same time, the lattice momentum $2\pi/a_0$ is large resulting in $\omega_s(2\pi/a_0)$ being substantially different from ω_{JPR}.

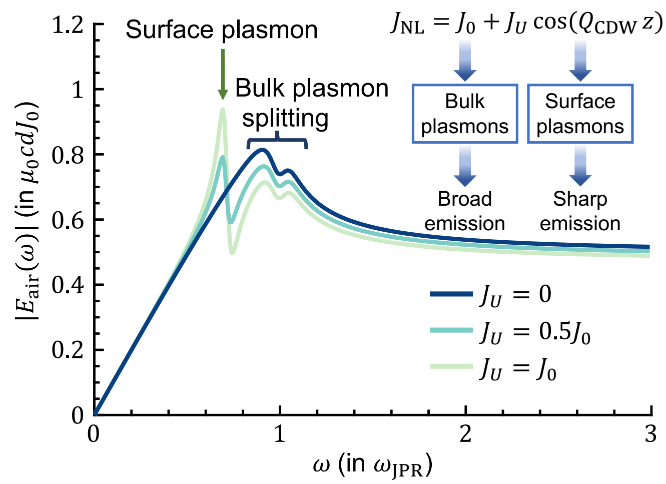

FIG. S3. Emission spectrum $f(\omega)$ in a system with $\omega_{ab} = \omega_c = 1\,\mathrm{THz}$, $\gamma_{ab} = \gamma_c = 0.1\,\mathrm{THz}$, $\varepsilon_{\infty,ab} = \varepsilon_{\infty,c} = 1$, $A = 0.1$. In such isotropic superconductors, bulk and surface resonances have notably different energies. This allows us to conclude that the homogeneous component J_0 of the photocurrent drives the bulk plasmons only, while the Umklapp one J_U affects the surface plasmons, in turn, providing a sharp resonant structure of $f(\omega)$.

Figure S2 shows the resulting dispersion $\omega_s(q_z)$. While at low momenta, $q_z \ll q_{\mathrm{TF}}$, we reproduce the same behavior as in Fig. 1(a), i.e., $\omega_s(q_z)$ shows a quick saturation near ω_{JPR}, at larger momenta, $\omega_s(q_z)$ becomes dispersive. In particular, for momenta $q_z \gtrsim q_{\mathrm{TF}}$, we expect that $\omega(q_z)$ will be substantially different from ω_{JPR}. The result in Fig. S2 implies that for the interpretation we offer in the main text to be consistent, in the experiment, we should have $Q_{\mathrm{CDW}} \lesssim q_{\mathrm{TF}} \lesssim 2\pi/a_0$ so that $\omega(Q_{\mathrm{CDW}}) \approx \omega_{\mathrm{JPR}}$. This latter requirement is essential from the perspective of back folding of the modes with momenta $q_z \simeq Q_{\mathrm{CDW}}$, which should have frequency close to ω_{JPR}.

IV. BULK VS SURFACE CONTRIBUTIONS TO THE SPECTRUM OF OUTGOING RADIATION

So far, we primarily studied strongly anisotropic superconductors with $\omega_{ab} \gg \omega_c$. A unique feature of such materials is that the surface modes saturate at the frequency immediately below the bulk Josephson plasmon resonance ω_{JPR}. This makes distinguishing whether the features in the spectral function of outgoing radiation arise from the surface or bulk modes difficult. To resolve this question, here we solve the problem for isotropic superconductors, where the surface plasmon frequency $\omega_{\mathrm{JPR}}/\sqrt{2}$ is well separated from the bulk.

Figure S3 shows the emission spectral function $f(\omega)$ in isotropic superconductors. For $J_U = 0$, $f(\omega)$ displays a double-peak structure near the bulk resonance: the dip that appears at ω_{JPR} corresponds to the bulk plasmon splitting in the striped phase due to the hybridization between zero and finite momentum bulk modes. Importantly, once $J_U \neq 0$, $f(\omega)$ exhibits an additional sharp peak at the surface resonance. This confirms both that the sharp resonance in Fig. 2 is due to the surface Josephson plasmons and that surface Josephson plasmons can only be resonantly excited by a nonzero Umklapp photocurrent. We remark that the bulk features are not severely renormalized by J_U. We conclude that the zero momentum photocurrent J_0 drives bulk modes and leads to a broad emission, while the Umklapp photocurrent J_U primarily drives surface excitations and leads to a sharp peak at the surface plasma resonance – see the inset in Fig. S3 for a summary.

V. REFLECTION FROM A MEDIUM WITH BRAGG MIXING

Here we compute the reflection coefficient r_p of the medium with stripes. Following the discussion in the main text, cf. Eqs. (9)-(10), we write the magnetic field as ($q_z = 0$):

$$B_{\mathrm{air},y} = [\alpha_a(e^{-k_a x} + r_p e^{k_a x}) + \beta_a e^{\tilde{k}_a x + iQz}]e^{-i\omega t}, \quad \text{(S23)}$$

$$B_{\mathrm{mat},y} = [\alpha_m e^{-\lambda_1 x}(1 + \gamma_1 e^{iQz}) + \beta_m e^{-\lambda_2 x}(\bar{\gamma}_2 + e^{iQz})]e^{-i\omega t}. \quad \text{(S24)}$$

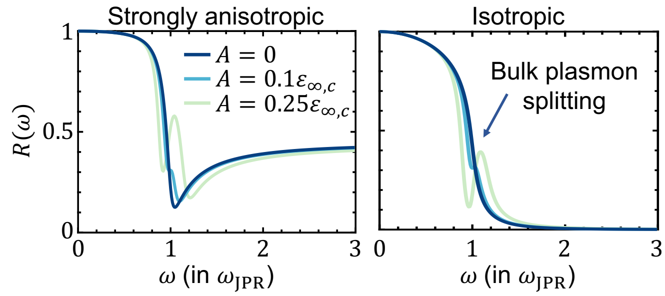

FIG. S4. Reflectivity $R(\omega)$ in anisotropic (left) and isotropic (right) superconductors with stripes. Provided the amplitude A of the CDW order is nonzero, there occur new features in $R(\omega)$ near the bulk plasmon resonance ω_{JPR}. At the same time, as indicated in the right panel, no features occur at the surface resonance, implying that the far-field photons are coupled only to the bulk plasmons. Parameters in the left (right) panel are the same as in Fig. 2 (Fig. S3).

Now, the coefficients $\alpha_a, \beta_a, \alpha_m, \beta_m$ are related to each through the appropriate Fresnel boundary conditions, which in turn give an implicit equation on r_p: $\det \mathcal{N} = 0$, where

$$\mathcal{N} = \begin{bmatrix} \frac{1}{r_p+1} + \frac{\varepsilon_c}{\varepsilon_c^2 - A^2}\frac{k_m^2}{\lambda_1 k_a}\frac{1}{r_p-1} & \left(\frac{1}{r_p+1} + \frac{\varepsilon_c}{\varepsilon_c^2 - A^2}\frac{k_m^2}{\lambda_2 k_a}\frac{1}{r_p-1}\right)\bar{\gamma}_2 \\ \left(1 + \frac{\varepsilon_c}{\varepsilon_c^2 - A^2}\frac{\tilde{k}_m^2}{\lambda_1 \tilde{k}_a}\right)\gamma_1 & 1 + \frac{\varepsilon_c}{\varepsilon_c^2 - A^2}\frac{\tilde{k}_m^2}{\lambda_2 \tilde{k}_a} \end{bmatrix}. \tag{S25}$$

For $A = 0$, we reproduce the familiar expression:

$$r_p = \frac{\varepsilon_c k_a - k_m}{\varepsilon_c k_a + k_m}. \tag{S26}$$

We compare the usual Josephson plasma edge appearing in the reflectivity spectra of a layered superconductor without stripes to reflectivity spectra renormalized by the stripes in Fig. S4 (left). We find that for $A \neq 0$, the Bragg mixing between zero momentum, $q_z = 0$, and finite momentum, $q_z = Q_{\mathrm{CDW}}$, gives rise to a plasma edge splitting. As shown in Fig. S4 (right), where following the preceding section, we consider isotropic superconductors and confirm that the new features in Fig. S4 (left) come from the bulk. In other words, far-field measurements, even in the presence of the CDW order, are sensitive to the bulk and not the surface excitations. However, up to relatively large stripe amplitudes, $A \sim 0.1\epsilon_{\infty,c}$, the new features appear negligible and can be easily missed within the experimental precision. This is consistent with reflectivity experiments in stripes which have reported only a single plasma edge. For this reason, in our calculations for terahertz emission, we use the value of $A = 0.1\epsilon_{\infty,c}$ as a reasonable upper limit to the stripe amplitude.

Notably, we find that the coupling to finite momentum modes can drastically enhance terahertz emission even though reflectivity probes are essentially insensitive to these modes up to large values of the stripe strength A.